Korean J. Chem. Eng., 40(6), 1268-1276 (2023)
DOI: 10.1007/s11814-023-1443-x
pISSN: 0256-1115
eISSN: 1975-7220

REVIEW PAPER

Hydrogenated amorphous carbon films deposited using plasma enhanced chemical vapor deposition processes

Jie Li*, and Heeyeop Chae**,***,†**

*Interuniversity Microelectronics Centre (IMEC), Heverlee, 3001, Belguim
**School of Chemical Engineering, Sungkyunkwan University (SKKU), Suwon 16419, Korea
***Sungkyunkwan Advanced Institute of Nanotechnology (SAINT), Sungkyunkwan University (SKKU), Suwon 16419, Korea
(*Received 15 December 2022 • Revised 29 January 2023 • Accepted 5 February 2023*)

Abstract−Hydrogenated amorphous carbon (a-C:H) is a class of amorphous carbon with more than 30% hydrogen content and containing sp^2 as well as sp^3 carbon atoms. It is widely used as a hard mask in semiconductor device fabrication, protective coatings, lubricants, and biomedical applications. The properties of a-C:H films are known to be strongly dependent on the carbon bonding structure and are characterized using the sp^2/sp^3 carbon hybridization ratio. The a-C:H films are typically deposited by plasma-enhanced chemical vapor deposition (PECVD) processes, and this review summarizes and discusses the relationship between the sp^2/sp^3 ratio of a-C:H and plasma characteristics. The effects of temperature, radical density, ion density, and ion energy on the sp^2/sp^3 ratio of a-C:H are investigated and summarized.

Keywords: Hydrogenated Amorphous Carbon, sp^2/sp^3 Ratio, Plasma Deposition, Plasma Characteristics

INTRODUCTION

Amorphous carbon (a-C) has been intensively studied for decades owing to its excellent characteristics, such as high mechanical hardness, chemical inertness, optical transparency, and low friction [1,2]. a-C can be classified based on the carbon bonding of the tetrahedral sp^3/trigonal sp^2 structure and hydrogen content. Typically, a-C is classified into three groups: hydrogen-free a-C, hydrogenated tetrahedral amorphous carbon (ta-C:H), and hydrogenated amorphous carbon (a-C:H), as shown in Fig. 1 [1].

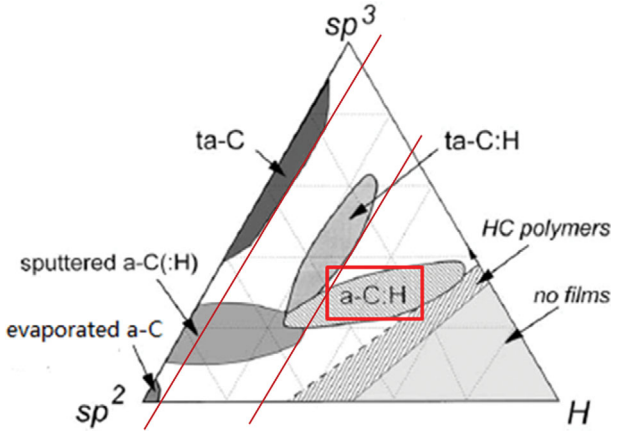

Fig. 1. Classification of amorphous carbon. Reproduced from ref. [1]. Copyright 2002 Elsevier.

Hydrogen-free a-C can be further divided into sp^2-rich hydrogen-free a-C (graphite-like a-C) and sp^3-rich hydrogen-free a-C (diamond-like a-C). Diamond-like a-C, also known as tetrahedral amorphous carbon (ta-C), is typically deposited by ionized evaporation, ion plating, or a beam containing carbon or hydrocarbon ions [3-5]. Diamond-like a-C, or ta-C, exhibits high density and hardness, and such good properties are attributed to the compact tetrahedral network of sp^3 carbon bonding. Graphite-like a-C is generally deposited by thermal evaporation or sputtering [1,3,5,6]. Graphite-like a-C shows a relatively low hardness due to weak intermolecular bonds within the trigonal structure of sp^2 carbon.

Hydrogenated tetrahedral amorphous carbon (ta-C:H) films with a limited hydrogen content (less than about 30%) are generally deposited using high-density plasma, such as microwave plasma and magnetically enhanced plasma [7-12]. The hardness of ta-C:H increases with an increased fraction of sp^3 carbon, similar to hydrogen-free a-C, and can be close to that of diamond-like a-C [7].

Hydrogenated amorphous carbon (a-C:H) with relatively high hydrogen content (approximately 30-55%) is deposited using plasma with a relatively low ion density [13-17]. The relatively low-density plasma for a-C:H deposition is often generated by radio-frequency inductively coupled plasma (ICP) or capacitively coupled plasma (CCP). These plasma sources are popular in the semiconductor fabrication industry. Certain properties of a-C:H, such as the film density and hardness, are determined by the carbon bonding structure and hydrogen content, as shown in Table 1. The sp^2-rich structure of a-C:H includes low hydrogen content and exhibits higher density and hardness, whereas the sp^3-rich structure includes high hydrogen content and exhibits lower density and hardness.

a-C:H is widely used as a hard mask in semiconductor device fabrication due to its easy processability and reasonable etch resistance [18-25]. As film patterning processes become finer in semi-

†To whom correspondence should be addressed.
E-mail: hchae@skku.edu

Table 1. Properties of a-C:H with different sp^2/sp^3 ratios [13-17]

Type of a-C:H	Hydrogen content (%)	sp^2/sp^3 structure	Density (g/cm^3)	Hardness (GPa)
Hard a-C:H	30-40	sp^2-rich	1.6-2.2	5-20
Soft a-C:H	40-55	sp^3-rich	1.2-1.6	3-5

conductor device fabrication, the exposure and development of conventional organic photoresists have been limited to making nano-scale patterns, especially in high-aspect-ratio etching processes [20,23,25]. a-C:H films are adopted because they have higher etch resistance and selectivity than organic photoresists, and the leftover a-C:H can be easily removed with O_2 plasma. a-C:H hard masks can be applied for patterning various SiO_2, SiN_x, SiON, and SiCOH films in semiconductor device fabrication processes [25-30]. The etch resistance of a-C:H hard mask is affected by carbon bonding structure and sp^2-rich a-C:H shows better resistance to fluorocarbon plasma and O_2 plasma than sp^3-rich a-C:H [19-22,24]. In this review, we examine the relationship between the process parameters of plasma processes and film properties. The sp^2/sp^3 ratio, hydrogen content, film hardness, optical band gap, and refractive index are summarized as functions of process parameters, and the effect of plasma characteristics on the sp^2/sp^3 ratio is discussed.

HYDROGEN CONTENT, sp^2/sp^3 RATIO, AND FILM PROPERTIES

Before discussing the relationship between the plasma characteristics and the sp^2/sp^3 ratio, the relationships between the sp^2/sp^3 ratio and hydrogen content, film hardness, optical band gap, and refractive index are summarized as shown in Fig. 2 [1,13-17]. The hydrogen content increases the sp^3 structure of a-C:H or reduces the sp^2/sp^3 ratio, as shown in Fig. 2(a). The film hardness increases with an increased sp^2/sp^3 ratio due to the compact structure with a reduced number of hydrogen atoms in the film, as shown in Fig. 2(b). No electrical band gap exists in amorphous carbon, but the optical band gap of a-C:H can be defined and determined experimentally from Tauc plotting [1,31]. The optical band gap decreases with an increased sp^2/sp^3 ratio due to the lower gap between the Π and Π^* states than that between the σ and σ^* states, as shown in Fig. 2(c). The refractive index of a-C:H film increases with the increase in sp^2/sp^3 ratio, as shown in Fig. 2(d), and this is attributed to the increased film density with an increased sp^2/sp^3 ratio [1].

The hydrogen content and sp^2/sp^3 ratio of the a-C:H film are measured by various metrological methods. Hydrogen content can be estimated using nuclear magnetic resonance (NMR) spectroscopy, nuclear reaction analysis (NRA), second ion mass spectrometry (SIMS), and infrared spectroscopy [13,15,32-34]. The sp^2/sp^3 ratio can be determined with NMR, X-ray photoelectron spectroscopy (XPS), and electron energy loss spectroscopy (EELS) [15,35-38], and is also indicated by the intensity ratio of the D peak to the G peak (I_D/I_G) in Raman spectra [19]. The I_D/I_G ratios are linearly dependent on sp^2/sp^3 ratios, as shown in Fig. 3.

a-C:H films of various sp^2/sp^3 ratios, hydrogen content, and film properties have been deposited using different plasma sources, including ICP, CCP, and electron cyclotron resonance (ECR) plas-

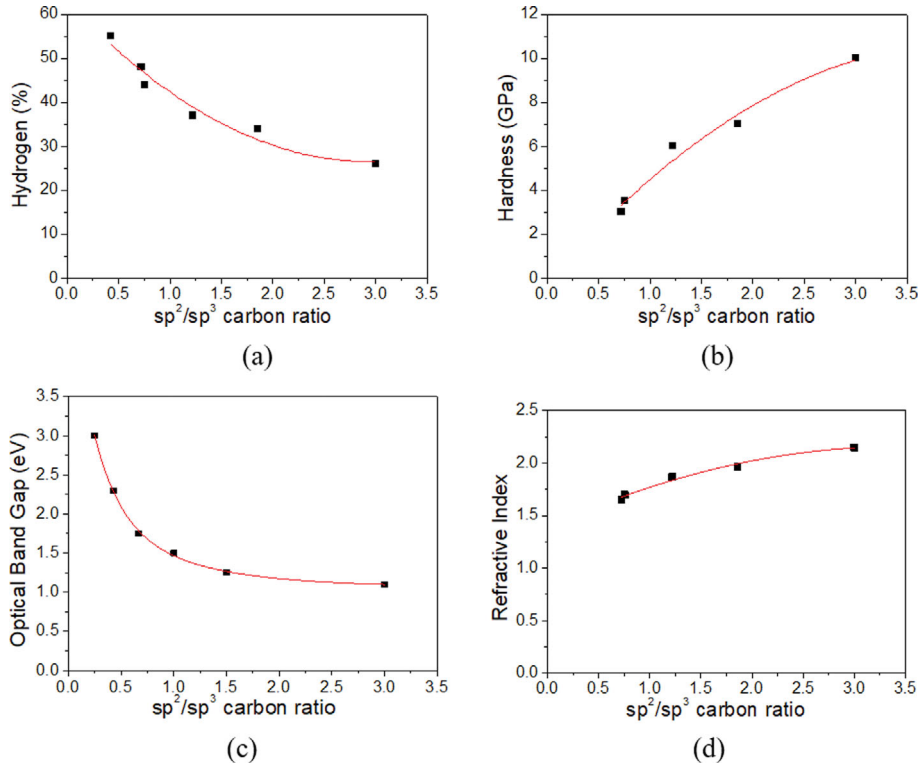

Fig. 2. The effect of sp^2/sp^3 ratio on (a) hydrogen content, (b) film hardness, (c) optical band gap, and (d) refractive index. (a) and (b) reproduced from ref. [15]. Copyright 1991 American Institute of Physics. (c) and (d) reproduced from ref. [1]. Copyright 2002 Elsevier.

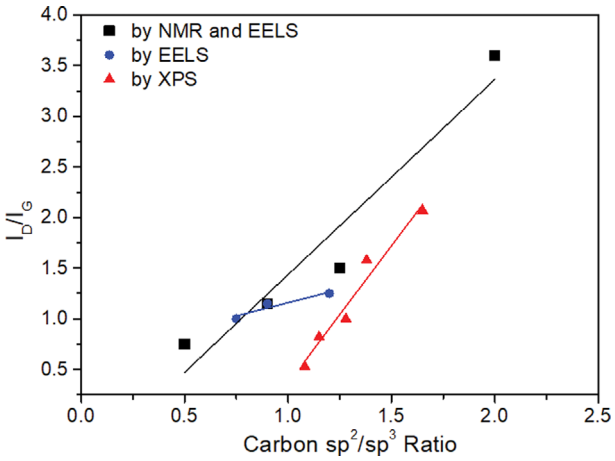

Fig. 3. The I_D/I_G ratios of a-C:H films as a function of sp^2/sp^3 ratio from NMR, EELS, and XPS. Reproduced from ref. [19]. Copyright 2021 Elsevier.

mas, with various hydrocarbon precursors such as CH_4 and C_2H_2. In this review, the correlation between the sp^2/sp^3 ratio of a-C:H and plasma conditions such as temperature, radical density, ion density, and ion energy is discussed as follows.

EFFECT OF TEMPERATURE ON sp^2/sp^3 RATIO OF a-C:H

The processing temperature is undoubtedly a vital process variable, and the effects of temperature on hydrogen content and sp^2/sp^3 ratio during film deposition processing or after deposition are summarized, as shown in Table 2 and Fig. 4 [19,22,32,35,36,39-41]. The hydrogen content decreases with increased substrate temperature in C_2H_2 plasma because high temperatures can remove hydrogen by forming volatile H_2, as shown in Fig. 4(a) [32]. The effect of temperature on the sp^2/sp^3 ratio of a-C:H is summarized. The I_D/I_G ratio in Raman spectra increases with increased substrate temperature in C_2H_2 plasma, as shown in Fig. 4(b), and with increased gas-phase temperature in C_3H_6 and C_6H_{12} plasmas, shown in Fig. 4(c) [19,22,41]. The sp^2/sp^3 ratio also increases with the post-annealing temperature after a-C:H film deposition by CH_4 plasma, as shown in Fig. 4(d) [35,36]. A high processing temperature or a thermal annealing after deposition can remove hydrogen atoms from the film and transform carbons from sp^3 to sp^2 bonding. The sp^2/sp^3 ratio difference of a-C:H in Fig. 4(d) is attributed to the different deposition conditions. The variations in film properties, such as hardness and optical band gap, are also summarized as follows. The film hardness increases with an increase in substrate temperature due to the compact carbon network with low hydrogen content, as shown in Fig. 4(e) [39]. The optical band gap decreases with increased substrate temperature due to the lower gap between the Π and Π* states with a high sp^2 fraction, as shown in Fig. 4(f) [40]. In conclusion, a high temperature results in low hydrogen content and a high sp^2/sp^3 ratio during film deposition or the post-annealing process.

EFFECT OF CHEMISTRY AND DENSITY OF RADICALS ON sp^2/sp^3 RATIO OF a-C:H

The hydrocarbon radicals in deposition plasma are important for determining the sp^2/sp^3 ratio of a-C:H film. The species of hydrocarbon radicals are determined by precursors, and their effect on the sp^2/sp^3 ratio is summarized in Table 3 and Fig. 5 [19,32-34,42]. The a-C:H film deposited using CH_4 plasma shows a higher hydrogen content than that deposited using C_2H_2 plasma. This is due to the presence of hydrogen-rich radicals in CH_4 plasma compared to carbon-rich radicals in C_2H_2 plasma, as shown in Fig. 5(a) [33]. The CH_4 plasma-deposited a-C:H film also shows a lower refractive index than the C_2H_2 plasma-deposited film because of the higher hydrogen content and lower film density, as shown in Fig. 5(b) [33,42]. The plasma chemistry can also be affected by pressure. The hydrogen content of a-C:H deposited using C_2H_2 ICP and CCP plasmas increases with high pressure, as shown in Fig. 5(c) and 5(d) [32,34], while that deposited using CH_4 CCP plasmas has an unchanged hydrogen content with different pressures (Fig. 5(d)) [34]. This is possibly because, with increased pressure, H atoms recombine with carbon-rich radicals in C_2H_2 plasma and increase the H/C ratio, leaving behind a higher film hydrogen content. However, in CH_4 plasma, a large number of H atoms are present, which tend to recombine with other H atoms to form H_2, barely affecting the H/C ratio of hydrogen-rich radicals. The I_D/I_G ratio decreases with an increase in the pressure of C_2H_2 ICP plasma, as shown in Fig. 5(e) [19]. The low sp^2/sp^3 ratio is attributed to the high film hydrogen content and high sp^3 fraction. The refractive index of a-C:H deposited using C_2H_2 plasma decreases with in-

Table 2. Plasma deposition of a-C:H at different temperatures

Process parameter	Plasma source	Precursor	Temperature (°C)	Analyzed property	Reference
Substrate temperature or gas-phase temperature	ICP	C_2H_2	100-500	Hydrogen content (32-47%)	[32]
	ICP	C_2H_2	45-77	I_D/I_G	[19]
	CCP	C_3H_6, C_6H_{12}	350-550	I_D/I_G	[22]
	CCP	C_6H_{12}	350-550	I_D/I_G	[41]
	CCP	CH_4	−23-147	Hardness	[39]
	ECR	CH_4	25-400	Optical band gap	[40]
Post-annealing temperature	CCP	CH_4	280-520	sp^2/sp^3 ratio (0.2-0.56)	[35]
	CCP	CH_4	220-700	sp^2/sp^3 ratio (0.94-1.29)	[36]

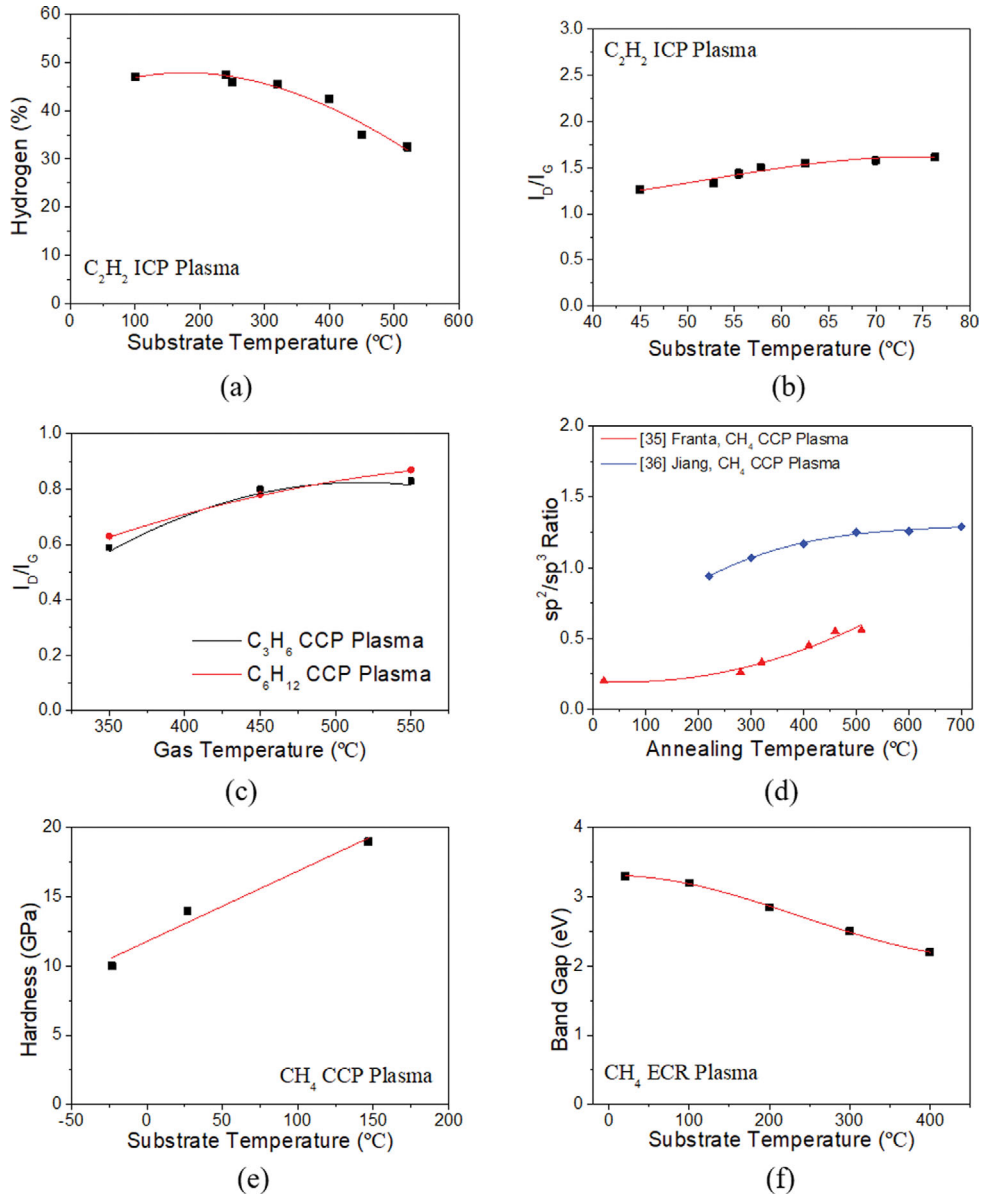

Fig. 4. (a) The effect of substrate temperature on hydrogen content. Reproduced from ref. [32]. Copyright 1990 Elsevier. I_D/I_G ratios with (b) various substrate temperatures (reproduced from ref. [19] with copyright 2021 Elsevier) and (c) gas-phase temperatures (reproduced from ref. [22] with copyright 2011 Elsevier). (d) Effect of annealing temperature on sp^2/sp^3 ratio. Reproduced from ref. [35] with copyright 2005 Elsevier and ref. [36] with copyright 2019 Elsevier. Effect of substrate temperature on (e) hardness (reproduced from ref. [39] with copyright 2004 Elsevier) and (f) optical band gap (reproduced from ref. [40] with copyright 1997 Elsevier).

Table 3. Plasma deposition of a-C:H with different radical chemistry and density

Process parameter	Plasma source	Precursor	Analyzed property	Reference
Precursor	CCP	CH_4, C_2H_2	Hydrogen content (23-36%)	[34]
	ECR	CH_4, C_2H_2	Hydrogen content (30-62%)	[33]
	ECR	CH_4, C_2H_2	Refractive index	[42]
Pressure	ICP	C_2H_2	Hydrogen content (28-42%)	[32]
	ICP	C_2H_2	I_D/I_G	[19]
	ECR	CH_4, C_2H_2	Refractive index	[33]
Radical density	ICP	C_2H_2	I_D/I_G	[19]

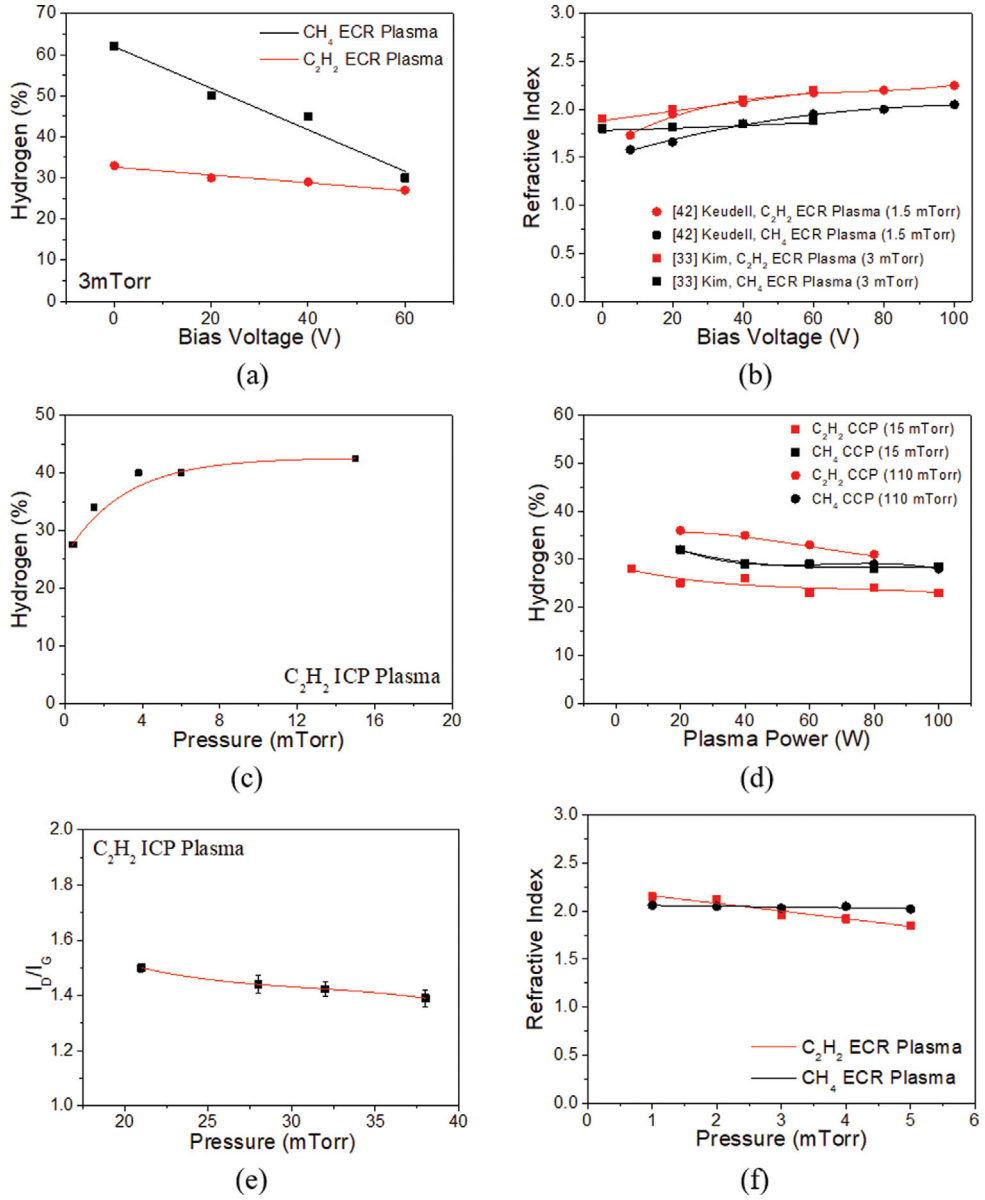

Fig. 5. (a) Hydrogen content (reproduced from ref. [33] with copyright 2000 Elsevier) and (b) refractive index of a-C:H (reproduced from ref. [33] with copyright 2000 Elsevier and ref. [42] with copyright 1997 American Institute of Physics) deposited using ECR plasmas with precursors of CH_4 and C_2H_2. (c) The effect of pressure on hydrogen content in ICP C_2H_2 plasma. Reproduced from ref. [32]. Copyright 1990 Elsevier. (d) Hydrogen content of a-C:H deposited using CCP plasmas with precursors of CH_4 and C_2H_2. Reproduced from ref. [34]. Copyright 2007 American Institute of Physics. (e) The effect of pressure on I_D/I_G ratio in ICP C_2H_2 plasma. Reproduced from ref. [19]. Copyright 2021 Elsevier. (f) Refractive index as a function of pressure in ECR plasmas with precursors of CH_4 and C_2H_2. Reproduced from ref. [33]. Copyright 2000 Elsevier.

creased pressure because of its higher film hydrogen content and lower film density. In contrast, that deposited using CH_4 plasma is almost constant, as shown in Fig. 5(f) [33].

The hydrocarbon radical density influences the sp^2/sp^3 ratio of a-C:H. The CH radical density in C_2H_2 ICP plasma was estimated by optical actinometry and directly correlated with the sp^2/sp^3 ratio [19]. The I_D/I_G ratio decreases with increased CH radical density under different source power, pressure, and substrate temperature conditions, as shown in Fig. 6. Compared with other dominant radicals, such as C_2 and C_2H in C_2H_2 plasmas, the addition of hydrogen-rich CH radicals on a film surface can introduce more hydrogen atoms into the film during a-C:H growth. Therefore, the high density of CH radicals increases the H/C ratio in plasma as well as film hydrogen content, lowering the sp^2/sp^3 ratio.

EFFECT OF ION DENSITY AND ENERGY ON sp^2/sp^3 RATIO OF a-C:H

1. Ion Density Effect

Apart from the processing temperature and plasma chemistry,

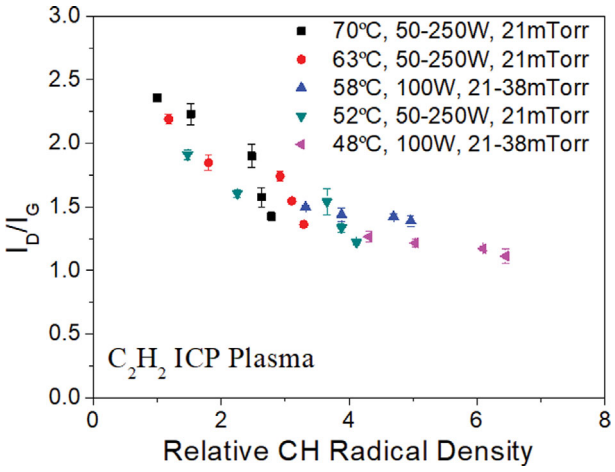

Fig. 6. The effect of CH radical density on I_D/I_G ratio under various C_2H_2 ICP plasma conditions. Reproduced from ref. [19]. Copyright 2021 Elsevier.

ion bombardment during the plasma deposition process also strongly affects the sp^2/sp^3 ratio of the a-C:H film. The effect of ion bombardment on the sp^2/sp^3 ratio can be explained in terms of ion density and ion energy. a-C:H films of various sp^2/sp^3 ratios, hydrogen content, and film hardness have been deposited in ICP plasmas with different source powers. The effects of ion density on hydrogen content and sp^2/sp^3 ratio are summarized in Table 4 and Fig. 7 [19,32,37,43]. The hydrogen content decreases with an increase in the source power of C_2H_2 ICP plasma, as shown in Fig. 7(a) [32], and the I_D/I_G ratio increases with the source power of C_2H_2 ICP plasma, as shown in Fig. 7(b) [19]. The increased number of ions in high-source-power ICP plasma can remove hydrogen atoms from C-H bonds in films and increase the sp^2/sp^3 ratio. The I_D/I_G ratio is correlated with ion density during deposition processes, as shown in Fig. 7(c) [19]. It increases with ion density under different substrate temperatures, plasma source powers, and pressures in C_2H_2 ICP plasmas. The sp^2/sp^3 ratio also increases with ion dose when a-C:H is irradiated by Ar ions after film deposition, as shown in Fig. 7(d) [37]. The increased sp^2/sp^3 ratio with ion density/ion dose indicates that ion bombardment can remove hydrogen and increase the sp^2 fraction during plasma deposition, and after film deposition. The film hardness increases with the increase in CH_4 ICP plasma source power due to the low hydrogen content and compact carbon network, as shown in Fig. 7(e) [43]. In conclusion, ion bombardment can remove hydrogen atoms and increase the sp^2/sp^3 ratio during or after deposition, and high ion density leads to a high sp^2/sp^3 ratio.

2. Ion Energy Effect

The effect of ion energy on the sp^2/sp^3 ratio is summarized, as shown in Table 5 and Fig. 8 [13,15,33,38,42,44]. a-C:H films of different sp^2/sp^3 ratios, hydrogen content, and refractive indices have been deposited using hydrocarbon plasmas from various plasma sources, including ICP, CCP, and ECR. The ion energy in plasma can be adjusted by the bias power or bias voltage. The hydrogen content decreases with increased bias voltage in CH_4 and C_6H_6 CCP plasmas (Fig. 8(a)) and also in CH_4 and C_2H_2 ECR plasmas (Fig. 8(b)) because high-energy ions can remove hydrogen atoms from a-C:H films [13,15,33]. The higher hydrogen content of a-C:H deposited using CH_4 plasma compared to that deposited using C_2H_2, and C_6H_6 plasmas is attributed to hydrogen-rich radicals in CH_4 plasma. The effect of ion energy on the sp^2/sp^3 ratio is summarized as follows. The I_D/I_G ratio increases with the increase in bias power of C_3H_6 ICP, as shown in Fig. 8(c) [44], and the sp^2/sp^3 ratio increases with the increase in bias voltage of CH_4 and C_2H_2 CCP plasmas, as shown in Fig. 8(d) [15,38]. The high sp^2/sp^3 ratio is attributed to high-energy ions that remove hydrogen atoms, both from the surface of a-C:H films by sputtering and from bulk

Table 4. Plasma deposition of a-C:H with different ion density

Process parameter	Plasma source	Precursor	Analyzed property	Reference
Source power	ICP	C_2H_2	Hydrogen content (21-26%)	[32]
	ICP	C_2H_2	I_D/I_G	[19]
	ICP	CH_4	Hardness	[43]
Ion density	ICP	C_2H_2	I_D/I_G	[19]
Ion irradiation dose	ICP	C_2H_2	sp^2/sp^3 ratio (0.9-8)	[37]

Table 5. Plasma deposition of a-C:H with different ion energy

Process parameter	Plasma source	Precursor	Analyzed properties	Reference
Bias power	ICP	C_3H_6	I_D/I_G	[44]
Bias voltage	CCP	CH_4	sp^2/sp^3 ratio (0.8-3), hydrogen content (30-44%)	[15]
	CCP	CH_4	sp^2/sp^3 ratio (0.3-1.4)	[38]
	CCP	C_6H_6	Hydrogen content (24-40%)	[13]
	ECR	CH_4, C_2H_2	Hydrogen content (30-62%)	[33]
	ECR	CH_4, C_2H_2	Refractive index	[42]

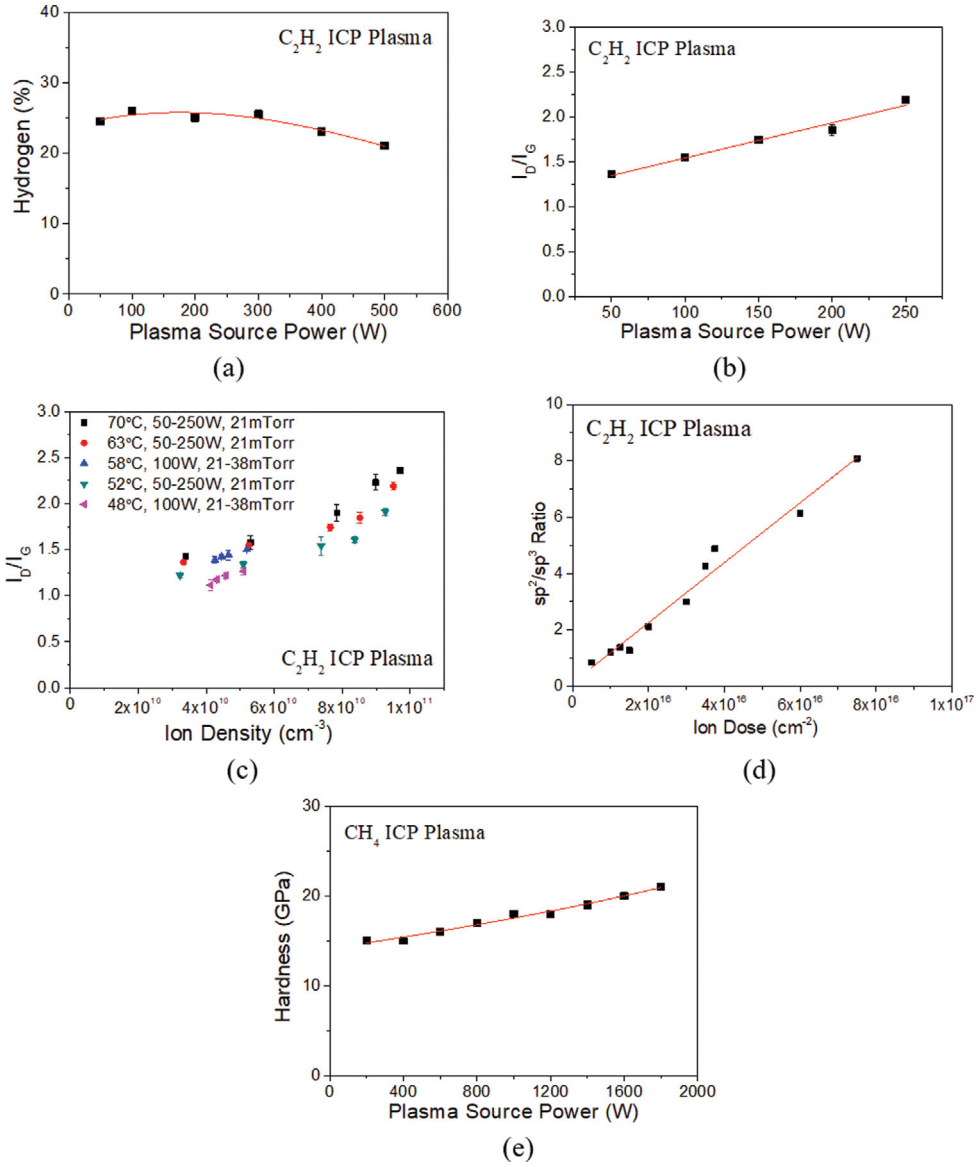

Fig. 7. Effect of plasma source power on (a) hydrogen content (reproduced from ref. [32] with copyright 1990 Elsevier) and (b) I_D/I_G ratio (reproduced from ref. [19] with copyright 2021 Elsevier). (c) Effect of ion density on I_D/I_G ratio under various C_2H_2 plasma conditions. Reproduced from ref. [19]. Copyright 2021 Elsevier. (d) sp^2/sp^3 ratio with 2.75 keV Ar ion bombardment of different doses after film deposition. Reproduced from ref. [37]. Copyright 1993 Elsevier. (e) Effect of plasma source power on film hardness. Reproduced from ref. [43]. Copyright 2002 Elsevier.

films through penetration. Thus, energetic ions reduce the hydrogen content of a-C:H and increase the sp^2/sp^3 ratio. Furthermore, inelastic collisions between energetic ions and carbon atoms can dissipate excessive ion energy as heat and transform sp^3 into sp^2 carbon [1]. The different sp^2/sp^3 ratios of a-C:H films deposited using CH_4 CCP plasmas in two separate studies [15,38] were possibly caused by the different reactor setups, as shown in Fig. 8(d). The refractive index of a-C:H increases with bias voltages in CH_4 and C_2H_2 plasmas, as shown in Fig. 8(e) [42]. The high refractive index obtained with high ion energy is due to the high carbon film density with low hydrogen content. The lower refractive index obtained with CH_4 plasma than with C_2H_2 plasma is attributed to the hydrogen-rich radicals in CH_4 plasma. In conclusion, plasmas having high ion energy can produce a-C:H thin films with low hydrogen content and a high sp^2/sp^3 ratio.

CONCLUSION

Various studies on the plasma deposition of a-C:H thin films were reviewed. We have summarized the effects of process parameters, such as the processing temperature, annealing temperature, pressure, source power, and bias power, on hydrogen content, the sp^2/sp^3 ratio, and film properties. The relationships between the sp^2/sp^3 ratio of a-C:H and the plasma characteristics of temperature, radical density, ion density, and ion energy were discussed. High temperature removes hydrogen atoms from C-H bonds and in-

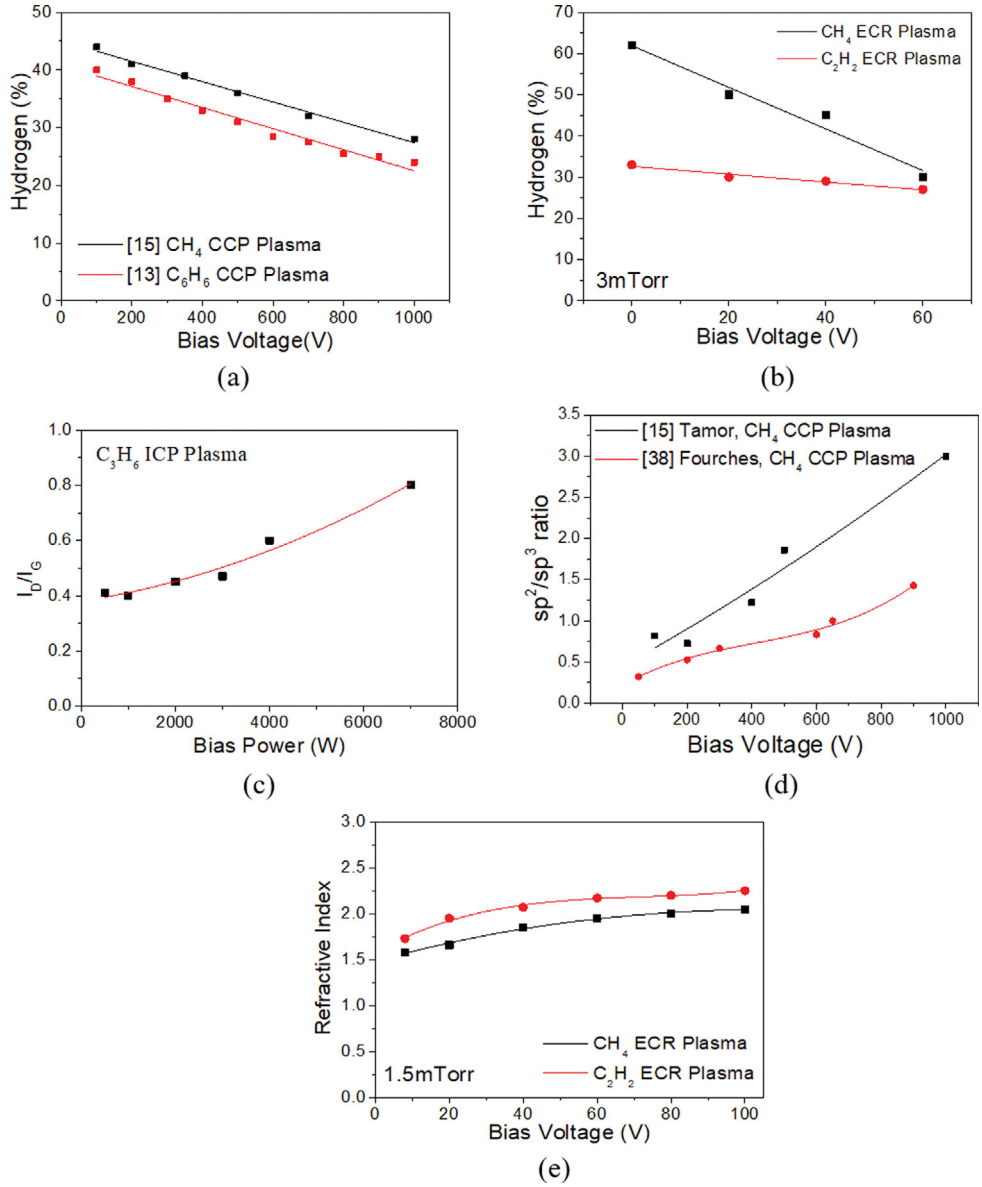

Fig. 8. Hydrogen content with various bias voltages in (a) CCP and (b) ECR plasmas. (a) reproduced from ref. [13] with copyright 1990 Trans Tech Publications and ref. [15] with copyright 1991 American Institute of Physics. (b) reproduced from ref. [33] with copyright 2000 Elsevier. (c) Effect of bias power on I_D/I_G ratio. Reproduced from ref. [44]. Copyright 2018 Elsevier. (d) Effect of bias voltage on sp^2/sp^3 ratio. Reproduced from ref. [15] with copyright 1991 American Institute of Physics and ref. [38] with 1994 Elsevier. (e) Effect of bias voltage on refractive index. Reproduced from ref. [42]. Copyright 1997 American Institute of Physics.

creases the sp^2/sp^3 ratio. Hydrocarbon plasmas with high density of hydrogen-rich radicals increase hydrogen content and decrease the sp^2/sp^3 ratio. In contrast, those having high ion density and high ion energy produce a-C:H films with low hydrogen content and a high sp^2/sp^3 ratio.

ACKNOWLEDGEMENTS

This work was supported by the Korea Institute of Energy Technology Evaluation and Planning (KETEP) grant funded by the Korea Government Ministry of Trade, Industry, and Energy (No. 20172010104830), by a National Research Foundation of Korea (NRF) grant funded by the Korean government (MSIT) (No. 2018 R1A2A3074950), and by the Korea Institute for Advancement of Technology (KIAT) and the Ministry of Trade, Industry, & Energy (MOTIE) of the Republic of Korea (No. P0017363).

REFERENCES

1. J. Robertson, *Mater. Sci. Eng. R*, **37**, 129 (2002).
2. H. T. T. Vu, V. L. N. Vo and Y. Chung, *Korean J. Chem. Eng.*, **38**, 1139 (2021).
3. G. M. Pharr, D. L. Callahan, S. D. McAdams, T. Y. Tsui, S. Anders, A. Anders, J. W. Ager III, I. G. Brown, C. S. Bhatia, S. R. P. Silva

and J. Robertson, *Appl. Phys. Lett.*, **68**, 779 (1996).
4. D. R. McKenzie, *Rep. Prog. Phys.*, **59**, 1611 (1996).
5. N. Ohtake, M. Hiratsuka, K. Kanda, H. Akasaka, M. Tsujioka, K. Hirakuri, A. Hirata, T. Ohana, H. Inaba, M. Kano and H. Saitoh, *Materials*, **14**, 315 (2021).
6. J. Robertson, *Adv. Phys.*, **35**, 317 (1986).
7. M. Weiler, S. Sattel, K. Jung, H. Ehrhardt, V. S. Veerasamy and J. Robertson, *Appl. Phys. Lett.*, **64**, 2797 (1994).
8. J. Schwan, S. Ulrich, K. Jung, H. Ehrhardt, R. Samlenski and R. Brenn, *Diam. Relat. Mater.*, **4**, 304 (1995).
9. N. A. Morrison, S. E. Rodil, A. C. Ferrari, J. Robertson and W. I. Milne, *Thin Solid Films*, **337**, 71 (1999).
10. C. Baron, S. Ghodbane, A. Deneuville, T. E. Bustarret, L. Ortega and F. Jomard, *Diam. Relat. Mater.*, **14**, 949 (2005).
11. F. Piazza, O. Resto and G. Morell, *J. Appl. Phys.*, **102**, 013301 (2007).
12. S. Pisana, C. Casiraghi, A. C. Ferrari and J. Robertson, *Diam. Relat. Mater.*, **15**, 898 (2006).
13. P. Kiodl, C. Wild, B. Dischler, J. Wagner and M. Ramsteiner, *Mater. Sci. Forum*, **52**, 41 (1990).
14. J. W. Zou, K. Reichelt, K. Schmidt and B. Dischler, *J. Appl. Phys.*, **65**, 3914 (1989).
15. M. A. Tamor, W. C. Vassell and K. R. Carduner, *Appl. Phys. Lett.*, **58**, 592 (1991).
16. M. A. Tamor and W. C. Vassell, *J. Appl. Phys.*, **76**, 3823 (1994).
17. S.-C. Lee, F.-C. Tai and C.-H. Wei, *Mater. Trans.*, **48**, 2534 (2007).
18. K. P. Kim, W. S. Song, M. K. Park and S. J. Hong, *J. Nanosci. Nanotechnol.*, **21**, 2032 (2021).
19. J. Li, S. J. Kim, S. Han and H. Chae, *Surf. Coat. Technol.*, **422**, 127514 (2021).
20. J. Li, S. J. Kim, S. Han, Y. Kim and H. Chae, *Plasma Processes Polym.*, **18**, e2100075 (2021).
21. J. H. Kwon, S. Y. L. Park, K. C. Seo, W. J. Ban, G. O. Park and D. D. Lee, *Thin Solid Films*, **531**, 328 (2013).
22. S. Lee, J. Won, J. Choi, J. Park, Y. Jee, H. Lee and D. Byun, *Thin Solid Films*, **519**, 6683 (2011).
23. J. Li, Y. Kim, S. Han and H. Chae, *Materials*, **14**, 2941 (2021).
24. Z. Jiang, H. Zhu and Q. Sun, *Electronics*, **10**, 1374 (2021).
25. M. H. Jeon, J. W. Park, D. H. Yun, K. N. Kim and G. Y. Yeom, *J. Nanosci. Nanotechnol.*, **15**, 8577 (2015).
26. B. S. Kwon, J. S. Kim, N.-E. Lee and J. W. Shon, *J. Electrochem. Soc.*, **157**, D135 (2010).
27. S. Kim, G. Choi, H. Chae and N. E. Lee, *J. Nanosci. Nanotechnol.*, **16**, 5143 (2016).
28. B. Kwon, H. Lee, N. Lee, C. Kim and C. K. Choi, *J. Korean Phys. Soc.*, **62**, 67 (2013).
29. J. H. Lee, B. S. Kwon and N. E. Lee, *Thin Solid Films*, **521**, 83 (2012).
30. G. Choi, S. Kim, H. Jang, H. Chae and N. E. Lee, *J. Nanosci. Nanotechnol.*, **16**, 11817 (2016).
31. P. Makula, M. Pacia and W. Macyk, *J. Phys. Chem. Lett.*, **9**, 6814 (2018).
32. W. Dworschak, R. Kleber, A. Fuchs, B. Scheppat, G. Keller, K. Jung and H. Ehrhardt, *Thin Solid Films*, **189**, 257 (1990).
33. B. K. Kim and T. A. Grotjohn, *Diam. Relat. Mater.*, **9**, 37 (2000).
34. S. Peter, K. Graupner, D. Grambole and F. Richter, *J. Appl. Phys.*, **102**, 053304 (2007).
35. D. Franta, V. Bursikova, I. Ohlidal, L. Zajickova and P. Stahel, *Diam. Relat. Mater.*, **14**, 1795 (2005).
36. L. Jiang, T. Wang, Y. Peng, H. Tian, M. Li, T. Xiao, P. Xiang, Y. Sun and X. Tan, *J. Non-Cryst. Solids*, **514**, 60 (2019).
37. A. Fuchs, J. Scherer, K. Jung and H. Ehrhardt, *Thin Solid Films*, **232**, 51 (1993).
38. N. Fourches and G. Turban, *Thin Solid Films*, **240**, 28 (1994).
39. G. Capote, R. Prioli, P. M. Jardim, A. R. Zanatta, L. G. Jacobsohn and F. L. Freire Jr., *J. Non-Cryst. Solids*, **338**, 503 (2004).
40. S. F. Yoon, H. Yang, Rusli, J. Ahn, Q. Zhang and T. L. Poo, *Diam. Relat. Mater.*, **6**, 1683 (1997).
41. S. Lee, J. Won, J. Choi, S. Jang, Y. Jee, H. Lee and D. Byun, *Thin Solid Films*, **519**, 6737 (2011).
42. A. von Keudell and W. Jacob, *J. Appl. Phys.*, **81**, 1531 (1997).
43. Z. Sun, S. Xu and K. N. Ostrikov, *Diam. Relat. Mater.*, **11**, 92 (2002).
44. S. J. Park, D. Kim, S. Lee, Y. Ha, M. Lim and K. Kim, *Thin Solid Films*, **663**, 21 (2018).